Modification of Protein by Disulfide S-Monoxide and Disulfide S-Dioxide: Distinctive Effects on PKC†

Kuo-Ping Huang,*,‡ Freesia L. Huang,‡ Pavan K. Shetty,‡ and Alfred L. Yergey§

Section on Metabolic Regulation, Endocrinology and Reproduction Research Branch, and Laboratory of Cellular and Molecular Biophysics, National Institute of Child Health and Human Development, National Institutes of Health, Bethesda, Maryland 20892-4510

Received September 20, 2006; Revised Manuscript Received December 6, 2006

ABSTRACT: Disulfide S-monoxide (DSMO) and disulfide S-dioxide (DSDO) have been proposed as proximal mediators for the oxidant-mediated modification of proteins. These disulfide S-oxides (DSOs) derived from glutathione (GSH) and captopril (CPSH) were synthesized by iron- or methyltrioxorhenium (VII)-catalyzed oxidation of the thiols with H_2O_2. Treatment of mouse hippocampal extracts with [^{35}S]GS-DSOs revealed that a large number of proteins were susceptible to thionylation; however, only a limited number of the them were detectable by the commonly used antibody against GS-associated proteins. Using protein kinase C (PKC) as a model, we found that DSOs derived from different thiols modified this kinase with different efficacy and specificity; for example, the inhibitory potency of the kinase was glutathione disulfide S-dioxide (GS-DSDO) (IC_{50}, ∼30 μM) > captopril disulfide S-dioxide (CPS-DSDO) (IC_{50}, ∼450 μM) > glutathione disulfide S-monoxide (GS-DSMO) and captopril disulfide S-monoxide (CPS-DSMO). The stoichiometries of thionylation of PKC β mediated by [^{35}S]GS-DSMO and [^{35}S]GS-DSDO were approximately 1 and 5 mol/mol, respectively, and at least four glutathionylation sites were identified in the GS-DSDO-treated kinase. Modification of PKC by GS-DSDO and CPS-DSDO rendered the kinase very susceptible to limited proteolysis; the former preferentially caused the degradation of the catalytic and the latter the regulatory domain of the kinase. Furthermore, CPS-DSDO-mediated modification of PKC increased the autonomous kinase activity; this was not the case for GS-DSDO-mediated modification. Since DSOs of different oxidative states as well as those derived from different thiols exert different effects on a target protein, these molecules could cause distinct cellular responses if derived from endogenous cellular reactions or even if they arise from exogenous sources.

Redox modification of protein by the abundant cellular thiol, glutathione (GSH),[1] provides a mechanism for the alteration of protein function similar to the phosphorylation/dephosphorylation catalyzed by protein kinases and phosphatases. Even though many enzymes, transcriptional factors, cell surface receptors, and cytoskeletal proteins have been shown to be thionylated (*1*, *2*), the full extent of this regulatory mechanism has not yet been fully explored. Modification of proteins by oxidized GSH-derivatives is generally believed to be nonenzymatic, whereas reduction of the oxidized protein has been proposed to be mediated by thiol-disulfide exchange and by glutaredoxin and thioredoxin reductase (*3*). The most recognizable form of the oxidized GSH, glutathione disulfide (GSSG), is rather inert and mostly involved in thiol-disulfide exchange reaction. Previously, we showed that treatment of rat brain slices with oxidants caused neurogranin to be thionylated as well as forming intramolecular disulfide (*4*). It was speculated that these oxidant-mediated modifications of protein were partially triggered by two highly reactive disulfide S-oxides (DSOs), glutathione disulfide *S*-monoxide (GS-DSMO) and glutathione disulfide S-dioxide (GS-DSDO). These two DSOs were detected in the oxidant-treated rat brain slices labeled with [^{35}S]cysteine. GS-DSMO and GS-DSDO were originally identified as degradation products of S-nitrosoglutathione in aqueous solution (*4*). DSOs are generally believed to be very reactive to nucleophiles, especially to the thiolate anion (RS^-), forming mixed disulfides. Natural products, such as allicin (diallyldisulfide S-monoxide, a DSMO) from garlic and S-methyl methanethiosulfonate ($CH_3S(O)_2SCH_3$, a DSDO) from cabbage and cauliflower have been studied for many years for their antimicrobial and beneficial health effects (*5*−*8*).

In this study, we synthesized DSOs from GSH and captopril (D-2-methyl-3-mercaptopropanoyl-L-proline) (CPSH), an angiotensin-converting enzyme inhibitor, to investigate their efficacy and specificity to modify proteins. Captopril

† This research was supported by the Intramural Research Program of National Institute of Child Health and Human Development, NIH.

* To whom correspondence should be addressed. Building 49, Room 6A36, NIH, Bethesda, MD 20892-4510. Telephone: (301) 496-7827. Fax: (301) 496-7434. E-mail: huangk@mail.nih.gov.

‡ Section on Metabolic Regulation, Endocrinology and Reproduction Research Branch.

§ Laboratory of Cellular and Molecular Biophysics, National Institute of Child Health and Human Development.

[1] Abbreviations: GSH, glutathione; GSSG, glutathione disulfide; DSO, disulfide S-oxide; DSMO, disulfide S-monoxide; DSDO, disulfide S-dioxide; DTNB, 5,5′-dithiobis(2-nitrobenzoic acid); CPSH, captopril; BSA, bovine serum albumin; DTPA, diethylenetriaminepentaacetic acid; MTO, methyltrioxorhenium (VII); MNB, 5-mercapto-2-nitrobenzoate; ES-MS, electrospray ionization mass spectrometry; GSNO, S-nitrosoglutathione.

10.1021/bi061955i
Published on Web 01/24/2007

is a widely used anti-hypertensive drug, which also has antioxidant activity (*9*). Patients taking this drug are known to have their serum albumin thionylated (*10*). Using protein kinase C (PKC) as a model, we showed that the synthetic DSOs of different oxidative states, DSMO vs DSDO, and those derived from different thiols, GSH vs CPSH, exhibited distinct effects on PKC. These findings suggest that DSOs from a variety of thiols may contribute to a broad range of redox regulation that has not previously been appreciated. The method described here for the preparation of DSOs will be useful for the characterization of protein modification mediated by a variety of thiols, including natural products and drugs.

MATERIALS AND METHODS

Materials. The following materials were obtained from the indicated sources: GSH, GSSG, CPSH, cysteine, cystine, homocysteine, diamide, 5,5′-dithiobis(2-nitrobenzoic acid) (DTNB), bovine serum albumin (BSA), trypsin, soybean trypsin inhibitor, diethylenetriaminepentaacetic acid (DTPA), iodoacetamide, and methyltrioxorhenium (VII) (MTO) from Sigma-Aldrich; S-nitrosoglutathione (GSNO) from Calbiochem; H_2O_2, ferric nitrate, and ferrous acetate from Fisher Scientific; [^{35}S]GSH from American Radiolabeled Chemicals Inc.; Microspin G-25 column from Amersham Biosciences; glyceraldehyde 3-phosphate dehydrogenase from Boehringer and Mannheim; mouse monoclonal antibody against glutathione−protein complexes from ViroGen: Bradford protein assay reagent, horseradish peroxidase-conjugated goat anti-mouse and rabbit antigoat IgG from Bio-Rad. Rat brain tubulin was a generous gift of Dr. Jan Wolfe, NIH.

Preparation of DSOs Derived from GSH and CPSH. GSH (50 mM) dissolved in water was incubated with H_2O_2 (100 mM) and MTO (0.5 mM) at room temperature for 30 min. The reaction mixture (400 μL) was injected into a C_{18} reverse phase HPLC column (connecting two Vydac 218TP510, 1.0 × 25 cm) and eluted with 0.1% TFA for 1 h at a flow rate of 1 mL/min, and the chromatography was monitored by the absorbance at 215 and 244 nm. DSOs derived from CPSH were prepared under the same incubation conditions as GSH. The reaction mixture was injected into a C_{18} reverse phase HPLC column (one Vydac 218TP510, 1.0 × 25 cm) and eluted with a linear gradient of 10−40% acetonitrile (in 0.1% TFA) for 30 min at a flow rate of 1 mL/min. Fractions of 0.5 mL were collected, lyophilized, and subjected to electrospray mass spectrometry (ES-MS) analysis. [^{35}S]-Labeled GS-DSOs were prepared by initial dilution of the radioactive GSH with non-radioactive GSH to a specific activity of ∼1000−2000 cpm/pmol and separated from DTT present in [^{35}S]GSH by HPLC on a C_{18} reverse phase column (connecting three Vydac 218TP54 columns, 0.46 × 25 cm, in tandem). The sample was eluted from the column with 0.1% TFA at a flow rate of 1 mL/min for 50 min. Pooled [^{35}S]GSH was lyophilized and incubated in 100 μL reaction mixture containing 1 mM [^{35}S]GSH, 3 mM H_2O_2, and 200 μM MTO for 20 min. The reaction products were separated by the same C_{18} column. The yields of GSO_2H + GSO_3H, GS-DSMO, and GS-DSDO were approximately 20−30% each and that of GSSG was less than 10%.

Determination of the Concentrations of DSOs. DSOs purified by HPLC were dissolved in water, and the concentrations were determined by titration with freshly prepared cysteine. The reaction mixture (50 μL) contained 50 mM sodium phosphate buffer (pH 7.2), 0.2 mM EDTA, 0.3 mM cysteine, and an increasing amount of DSOs. After incubation of the sample at room temperature for 10 min, 200 μL of DTNB solution (containing 0.25 M sodium phosphate buffer, pH 7.2, 1 mM EDTA, and 0.3 mM DTNB) was added, and the reduction in free −SH was measured spectrophotometrically at 410 nm. The reaction products of cysteine and DSOs were identified by HPLC and ES-MS. The predicted stoichiometry of reaction between DSMO and cysteine was 1:2 and that of DSDO and cysteine was 1:1.

Spectrophotometric Assay of Oxidation of 5-Mercapto-2-nitrobenzoate (*MNB*) *by DSOs.* The reactivities of DSOs toward the −SH group were determined by reaction with MNB derived from the reduction of DTNB with cysteine. The reaction mixture (250 μL), which contained 0.2 M sodium phosphate buffer (pH 7.2), 0.8 mM EDTA, 0.25 mM DTNB, and 60−70 μM cysteine, was incubated at room temperature for ∼5 min to generate MNB. A small volume of each DSO (<5 μL) was added, and the reaction was monitored by the oxidation of MNB, which resulted in a decrease in absorbance at 410 nm.

Modification of Proteins by DSOs. Protein samples (50−100 μL) were incubated in 10 mM potassium phosphate buffer, pH 7.5, containing 10% glycerol, and 2 mM DTT at room temperature for 30 min to reduce protein sulfhydryl groups. They were then loaded on top of G-25 Microspin columns, previously equilibrated with 20 mM potassium phosphate buffer, pH 7.2, containing 20% glycerol, and centrifuged at 5000 rpm for 7 s in an Eppendorf centrifuge to separate reduced proteins from DTT. Protein and residual DTT concentrations were determined before addition of DSMO and DSDO to the indicated concentrations, which were the net after subtraction of the free −SH in the samples. After the indicated times of incubation, iodoacetamide (final 10 mM) was added to stop the reaction, and samples were analyzed by nonreducing SDS−PAGE and/or immunoblot.

For measurement of PKC activity after modification with DSOs, iodoacetamide was omitted. Aliquots of PKC reaction mixtures (∼600 units, ∼1700 units/mg) were taken at timed intervals and diluted at least 10 times into the assay mixture containing 30 mM Tris-Cl buffer, pH 7.5, 6 mM $MgCl_2$, 0.12 mM [γ-^{32}P]ATP, 40 μM Ng28−43 peptide, and 100 μg/mL PS + 20 μg/mL DG + 0.4 mM $CaCl_2$ or 2 mM EGTA without Ca^{2+} and lipid activators. Assays were performed at 30 °C for 2 min, and ^{32}P-incorporation into the peptide substrate was measured by the Dowex AG1 × 8/DEAE-cellulose mini column method (*11*). A unit of PKC activity is defined as the amount of enzyme catalyzing the incorporation of 1 pmol of phosphate into the substrate per min. To determine the reversibility of DSO-mediated inactivation, DTT (10 mM) and $ZnSO_4$ (50 μM) were added at different time points. To determine the stoichiometry of thionylation, rat brain PKC β was incubated with 1 mM DTT on ice for 20 min to reduce the enzyme and was then separated from DTT by a G-25 Microspin colum. The enzyme (∼10−20 μg) was incubated with [^{35}S]GS-DSMO or [^{35}S]GS-DSDO at room temperature in 10 mM potassium phosphate buffer, pH 7.5, containing 10% glycerol, and aliquots were taken at timed intervals, precipitated with 20% TCA with the addition of 100 μg of BSA as carrier. After

the samples were subjected to centrifugation in a microcentrifuge at 14 000 rpm at 4 °C for 10 min, the pellet was washed once with 20% TCA and dissolved in 200 μL of 0.1 N NaOH for determining the radioactivity by scintillation counting with the addition of 10 mL of Bio-Safe II counting solution. For limited proteolysis, thionylated PKC (~10−15 μg) was incubated with trypsin (PKC/trypsin = 80) at room temperature, aliquots were taken at different times, and the reaction was terminated by soybean trypsin inhibitor (20 μg). Proteolyzed PKC was resolved by 8−16% nonreducing SDS−PAGE and transferred to nitrocellulose membrane, and thionylated PKC fragments were detected by autoradiography and, subsequently, immunoblotted with PKC polyclonal antibody (*12*). Alternatively, the proteolytic fragments of PKC were revealed by staining the gel with Coomassie blue. Rat brain Ca^{2+}/PS/DG-stimulated PKC α, β, and γ were purified from rat brain as previously described (*13*).

Immunoblot of Glutathionylated PKC. PKC (~1 μg) was incubated with DSOs at room temperature in 10 mM potassium phosphate buffer, pH 7.5, in duplicate for 5 min, and one set of the reaction mixture was terminated by the addition of iodoacetamide (13 mM) and the other by addition of DTT (10 mM) for 5 min followed by iodoacetamide (13 mM). To each of these reaction mixtures, SDS−PAGE sample buffer without mercaptoethanol was added, and proteins were resolved by 8−16% gradient SDS−PAGE. Proteins were transferred to nitrocellulose membrane and blotted with monoclonal antibody against GSH-associated protein (at 1:1000 dilution), HRP-conjugated goat anti-mouse IgG, and immunoreactive band revealed by ECL. The same membrane was stripped and blotted with goat anti-rat brain PKC antibody (*12*) to reveal the total amount of PKC applied. Those DSO-treated samples that were terminated by iodoacetamide alone represented the thionylated proteins and those terminated by DTT followed by iodoacetamide represented proteins whose modifications were reversed by DTT.

Identification of Modified Peptides. The tryptic peptides that were modified by GSH adduction were identified by MS/MS analysis of fragmentation spectra using MALDI TOF/TOF under unimolecular decomposition conditions. MALDI mass spectra of LC separated fractions of the labeled peptides were inspected for pairs of peptides differing in mass by 304 Da corresponding to loss or adduction of GSH. The pairs of candidate ions identified were subjected to fragmentation in a MALDI TOF/TOF instrument, and partial peptide sequences were reconstructed manually. The sequences derived were matched against the sequence of PKC β, and the full sequence of the tryptic peptide was deduced by locating a peptide that included both the derived sequence and matched peptide mass.

Mass Spectrometry. ES-MS was performed using M-Scan's Quattro II upgraded Bio-Q instrument with quadrupole analyzer for the identification of the various DSOs. Myoglobin was used to calibrate the instrument. Sample aliquots (10 μL) were injected into the instrument, and elution was carried out using a mixture of acetonitrile, 0.1% TFA, methoxyethanol, and isopropanol (1:1:1:1) at a flow rate of 5 μL/min. The spectra were deconvoluted, and the masses were expressed in daltons. MALDI MS and MS/MS analyses were carried out in a semi-automated fashion using an Applied Biosystems 4700 Proteomics analyzer with TOF/TOF ion optics (Applied Biosystems, Inc., Framingham, MA). In MS/MS mode the instrument was always operated with the collision gas off. All calibrations were performed only after allowing instrument voltages to stabilize for at least 60 min in the operation mode. Samples were prepared by spotting 0.3 μL of an LC separated tryptic digest fraction to the plate along with an equal volume of the matrix (α-cyano-4-hydroxycinnamic acid) solution (5 mg/mL recrystalized matrix in 1:1 0.1% TFA/acetonitrile with 10% 0.1 M $NH_4H_2PO_4$) and left to air-dry. The sample plate calibration file was updated for each plate using five spots of the ABI4700 Calibration Mixture. MS mode default calibration was updated daily using a calibration mixture spot in the center of the plate. MS/MS default calibration was updated based on successfully performing an internal calibration using the y-series fragment ions of Glu-Fibrinogen peptide, *m*/*z* 1570.677. MS spectra were obtained for each sample using 500 laser shots in MS mode and 3500 shots in MS/MS.

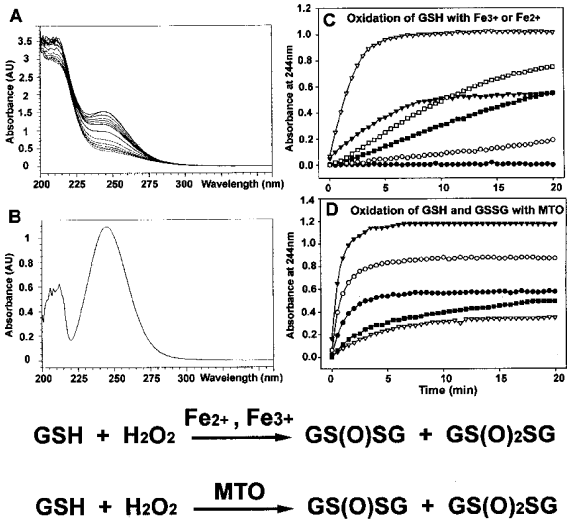

FIGURE 1: Absorption spectra of DSMO and the spectrophotometric assay of DSMO formation by oxidation of GSH with H_2O_2. (A) Absorption spectra of purified GS-DSMO (0.55 mM) in water exhibited a minor peak near 244 nm and upon addition of 2 mM cysteine the absorbance at this wavelength was progressively reduced. (B) The differential spectra of GS-DSMO before and after 20 min incubation with cysteine exhibited a peak near 244 nm. (C) GSH (2 mM) was incubated with 4 mM H_2O_2 in the presence of 40 (▼) and 80 μM (▽) Fe^{3+}, 40 (■) and 80 μM (□) Fe^{2+}, or without metal (○) and the absorbance at 244 nm was monitored. GSH alone without H_2O_2 or metal ion showed no change in the absorbance (●). (D) GSH (2 mM) was incubated with 4 mM H_2O_2 in the presence of 100 (●), 200 (○), and 400 μM (▼) MTO and GSSG (2 mM) was incubated with the same concentration of H_2O_2 in the presence of 200 (▽) and 400 μM (■) MTO. Absorbance at 244 nm was monitored.

RESULTS

Spectrophotometric Assay of DSOs Formation. Purified GS-DSMO displayed an absorption peak at 244 nm, which was not present in GSH and GSSG. Addition of cysteine to GS-DSMO resulted in the formation of GSH/cysteine mixed disulfide with a concomitant reduction in the absorbance at 244 nm (Figure 1A). The differential spectra of GS-DSMO and the GSH/cysteine mixed disulfide exhibited a peak at 244 nm (Figure 1B). Similarly, incubation of captopril disulfide S-monoxide (CPS-DSMO) with cysteine resulted in a reduction of absorbance at 244 nm. In the absence of

thiol, both GS-DSMO and CPS-DSMO were stable at neutral pH and reacted quantitatively with cysteine. The distinct absorbance of DSMO at 244 nm was not present in DSDOs, and its formation was determined by ES-MS following HPLC purification. Since DSMO is an initial product of oxidation of thiol with H_2O_2 and is converted to DSDO upon further oxidation, measurement of the increase in absorbance at 244 nm was used to optimize the condition for the oxidation of thiol or disulfide to form DSOs. Decomposition of DSMO has also been shown to lead to DSDO and the disulfide by a disproportionation process (*14*).

Recently, GS-DSMO and GS-DSDO was identified as decomposition products of GSNO (*4*, *15*). The rate of decomposition of GSNO at room temperature was slow and generated a variety of products including limited amount of DSOs. Previously, DSMOs were prepared by oxidation of disulfide with peracid (*16*−*18*) and GS-DSMO and GS-DSDO were shown to be generated by oxidation of GSH with H_2O_2 or other peroxides near neutral pH (*19*). However, reaction of thiol with H_2O_2 without catalyst is a relatively slow process and often requires a higher temperature (*18*). MTO has been shown to be an efficient catalyst for the oxidation of symmetric disulfides with H_2O_2 to form DSOs (*14*). To prepare these reactive sulfur species, we employed a spectrophotometric assay to optimize the conditions for the synthesis of these compounds. The rate of oxidation of GSH (2 mM) by H_2O_2 (4 mM) at room temperature, measured at absorbance of 244 nm, without metal ion was relatively slow, and the rate was greatly increased by iron (Figure 1C). The reaction catalyzed by Fe^{3+} was more efficient than that by Fe^{2+}. Similarly, Fe^{3+} was more effective than Fe^{2+} in catalyzing the oxidation of other thiols, including CPSH, cysteine, and homocysteine (data not shown). Oxidation of GSSG by H_2O_2 in the presence of Fe^{2+} or Fe^{3+} was much less efficient than that of GSH (data not shown). Both the Fe^{2+}- and Fe^{3+}-catalyzed reactions were inhibited by metal chelators, EDTA or DPTA.

The rate of MTO-catalyzed oxidation of thiol (2 mM) by H_2O_2 (4 mM) to form DSOs was also more efficient than that of disulfide (Figure 1D). MTO binds one or two molecules of H_2O_2 to form mono- and di-peroxides, respectively, and the rhenium-coordinated peroxides are activated for nucleophilic attack by a range of substrates, including alkyl and aryl sulfides (*20*). The sulfur atom in thiol apparently is a stronger nucleophile than that of the disulfide, and thus, the oxidation of thiol is faster than its disulfide as shown in this study. It is interesting to note that the amount of GS-DSMO formed in this reaction is positively correlated to the concentration of MTO. This phenomenon was also observed for the oxidation of CPSH with MTO. A parsimonious explanation of this observation is that the faster the oxidation of thiol to form DSMO the less the chance of consumption of DSMO by thiol to form disulfide and other compounds, which exhibit less absorbance at 244 nm. In contrast to the iron-catalyzed reaction, the MTO-catalyzed oxidation of thiol was insensitive to metal chelators, EDTA or DPTA.

Purification and Identification of the Oxidation Products of Thiols. The reaction products of oxidation of GSH by H_2O_2 and Fe^{3+} or MTO were separated by C_{18} reverse phase HPLC as previously described (*4*). The major products were identified by ES-MS as GS-DSMO [GS(O)SG, $m/z = 629.2$], GS-DSDO [$GS(O)_2SG$, $m/z = 645.1$], and GSSG ($m/z = 613.1$) (data not shown). The oxidation products of CPSH in the presence of H_2O_2 and Fe^{3+} (Figure 2A) or MTO (Figure 2B) were CPS-DSMO [CPS(O)SCP, $m/z = 449.1$], captopril disulfate S-dioxide (CPS-DSDO) [$CPS(O)_2CPS$, $m/z = 465.1$], and captopril disulfide (CPSSCP, $m/z = 433.1$) (Figure 2C). Other products that have been identified were sulfonic acid ($CPSO_3H$) ($m/z = 266.1$) and sulfinic acid ($CPSO_2H$, $m/z = 250.1$), both of which were eluted near the void volume. The Fe^{3+}-catalyzed oxidation of thiols generated a more complex array of products as compared to those by MTO and several of which had not been identified.

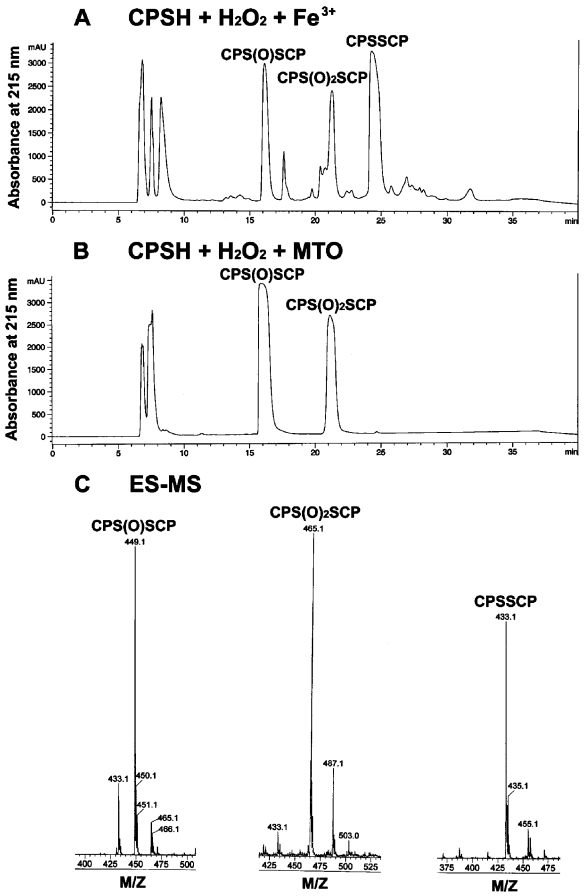

FIGURE 2: Identification of the reaction products derived from oxidation of CPSH with H_2O_2 catalyzed by Fe^{3+} or MTO. CPSH (50 mM) was incubated with H_2O_2 (100 mM) in the presence of 0.5 mM Fe^{3+} (A) or 0.5 mM MTO (B) for 30 min, the reaction mixture was injected into a C_{18}-reverse phase HPLC column, and the chromatography was monitored at 215 nm (see Experimental Procedures for details). Fractions were lyophilized and analyzed by ES-MS (C).

Reactivity of DSMO and DSDO toward Thiol. The reactions of GS-DSMO and GS-DSDO with MNB, which is derived from the reduction of DTNB with thiol, were monitored by the decrease in absorbance at 410 nm (Figure 3A). The reaction of GS-DSDO with MNB was instantaneous and immediately reached a steady state, indicating a very high reactivity of this compound toward thiol. When compared to the frequently used oxidant diamide, the rate of reaction of GS-DSMO (96 μM) with MNB (60 μM) was at least 2−3-times faster than that of diamide (96 μM) (Figure 3A). The reaction kinetics of CPS-DSDO with MNB were also very fast (Figure 3B) and similar to those of GS-DSDO and MNB, suggesting that these DSDOs are excellent

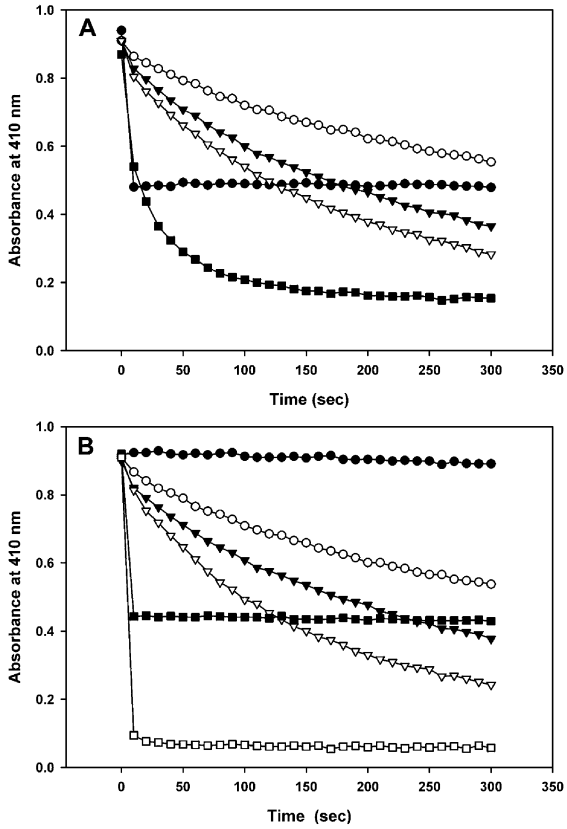

FIGURE 3: Rate of oxidation of MNB by CPS-DSMO, CPS-DSDO, GS-DSMO, GS-DSDO, and diamide. (A) MNB generated from 0.25 mM DTNB + 0.06 mM cysteine in 0.2 M sodium phosphate buffer, pH 7.2, was incubated with 32 μM GS-DSDO (●); 96 μM GS-DSMO (■); and 32 (○), 64 (▼), and 96 μM (▽) diamide. (B) MNB was incubated without the addition of DSO (●); with 32.5 (○), 65 (▼), and 97.5 μM (▽) CPS-DSMO; and 32.5 (■) and 65 μM (□) CPS-DSDO. Reaction of the sulfhydryl group of MNB with DSOs resulted in the formation of mixed disulfide with concomitant decrease in the absorbance at 410 nm.

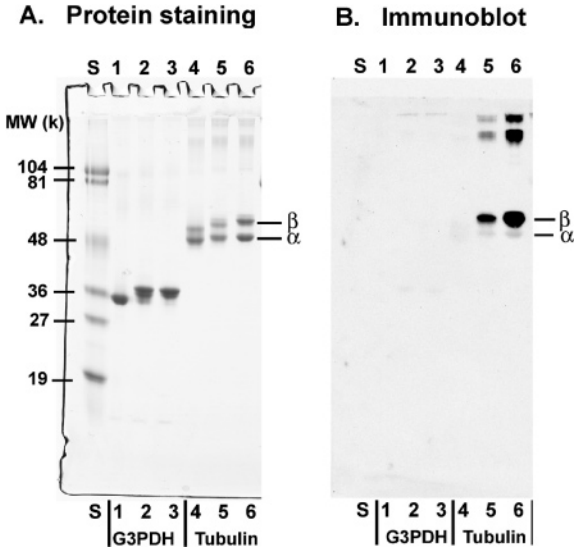

FIGURE 4: Thionylation of glyceraldehyde 3-phosphate dehydrogenase and rat brain tubulin with GS-DSMO and GS-DSDO. Reduced glyceraldehyde 3-phosphate dehydrogenase (G3PDH, 0.17 mg/mL) and tubulin (0.17 mg/mL) were incubated in 10 mM potassium phosphate buffer, pH 7.2, containing 10% glycerol, and 0.4 mM GS-GSMO (lanes 2 and 5) or 0.1 mM GS-DSDO (lanes 3 and 6) for 30 min. Samples (~3.5 μg of protein) were resolved by 8−16% nonreducing SDS−PAGE for protein staining with Coomassie blue (A) or immunoblot with monoclonal mouse anti-GS-protein antibody (B). Control samples were those without treatment with DSOs (lanes 1 and 4).

modifiers of −SH groups and form mixed disulfides quantitatively. The rate of reaction of GS-DSMO (96 μM) with MNB was 2−3-times faster than that of CPS-DSMO (97.5 μM), indicating that the reactivity of these compounds is not only dependent upon the functional group, S-monoxide, but also on other structure features of these molecules.

Oxidative Modification of Proteins by GS-DSMO and GS-DSDO. To test the efficacy of DSMO and DSDO in the modification of proteins, we initially employed antibody against GS-protein mixed disulfide for immunoblot analysis using glyceraldehyde 3-phosphate dehydrogenase (*15*, *21*, *22*) and tubulin (*23*) as substrates, both of which are known to be glutathionylated in oxidant-treated tissues. Treatment of these two proteins with either 0.1 mM GS-DSDO or 0.4 mM GS-DSMO resulted in a retarded electrophoretic mobility shift under nonreducing SDS−PAGE (Figure 4A). Immunoblot analysis with antibody against GS-protein (Figure 4B) showed a stronger reactivity toward the GS-DSDO-treated tubulin and a much lower response to that treated with GS-DSMO; this suggests that GS-DSDO is more reactive than GS-DSMO toward this protein. These DSOs can also thionylate polymerized tubulin. Although both the modified α and β subunits of tubulin exhibited retarded mobility shifts, only the latter showed a strong reactivity to the antibody. Both the GS-DSMO and the GS-DSDO-treated glyceraldehyde 3-phosphate dehydrogenase were poorly reactive toward GS-protein antibody. It is evident that this antibody has a restricted specificity toward glutathionylated proteins. To further investigate the specificity and efficacy of these DSOs on cellular proteins, we compared the incorporation of [^{35}S]GS-DSMO and -DSDO into mouse hippocampal extracts (Figure 5A). Incorporation of [^{35}S]GS from GS-DSDO (0.1 mM) into hippocampal proteins was more rapid and reached a level nearly three times that of GS-DSMO at 0.2 mM, indicating that the former is more reactive and possesses broader specificity. Autoradiography of the thionylated proteins, following nonreducing SDS−PAGE and transfer to a nitrocellulose membrane, revealed that a large number of proteins were thionylated by these DSOs (Figure 5B). These findings suggest that this type modification is widespread and may participate in a broad range of cellular regulation. Among these thionylated proteins detectable by autoradiography only a limited number were reactive toward the GS-protein antibody, its specificity was confirmed by the elimination of the majority of immunoreactive bands under reducing conditions (Figure 5C).

Modification of PKC by DSMO and DSDO. Since a variety of thiols are potential sources of DSOs, we compared the effect of DSOs derived from GSH and CPSH on PKC activity. All these compounds inhibited PKC activity with a potency order of GS-DSDO > CPS-DSDO > GS-DSMO and CPS-DSMO (Figure 6A). The IC_{50} for GS-DSDO and CPS-DSDO were approximately 30 and 450 μM, respectively. Even though CPS-DSDO had similar functional groups and reacted with MNB with equal effectiveness as GS-DSDO, the former was much less potent than the latter in inhibiting PKC. These findings demonstrate that DSOs derived from different thiols have distinctive effects on their target proteins. Both GS-DSMO and CPS-DSMO at concentrations less than 0.2 mM inhibited PKC poorly. The

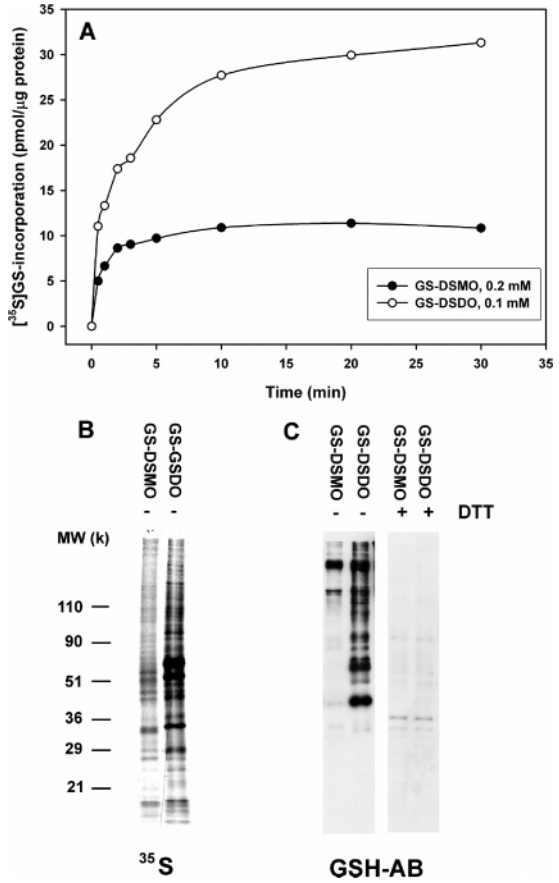

FIGURE 5: Glutathionylation of mouse brain hippocampal extracts with [^{35}S]GS-DSMO and [^{35}S]GS-DSDO. (A) Tissue extracts were incubated with 0.1 mM GS-DSDO (○) or 0.2 mM GS-DSMO (●) and samples were taken at timed intervals for the determination of [^{35}S]GS-incorporation into protein. (B) After 30 min incubation with DSOs, aliquots were taken for analysis by nonreducing SDS−PAGE, and proteins were transferred to nitrocellulose membrane for autoradiography. (C) Immunoblot analysis of DSO-treated samples with or without reduction by DTT using mouse monoclonal antibody against GS-associated proteins.

inhibitory effect of GS-DSMO over 0.4 mM varied greatly between different experiments. This unusual effect was not seen in CPS-DSMO. The unusual inhibitory effect of GS-DSMO on PKC could be in part due to glutathionylation of PKC as well as causing the kinase to form aggregates, which did not enter the 8−16% gradient nonreducing gel. The rate of inhibition mediated by 0.1 mM of GS-DSDO greatly exceeded that by 0.4 mM of GSSG or GSNO, two other potential glutathionylating agents (Figure 6B).

Glutathionylation of PKC by GS-DSDO and GS-DSMO could also be detected by immunoblot with a GS-protein specific antibody (Figure 6C, lower panel). The extent of thionylation by 0.1 mM GS-DSDO was comparable to that by the combination of 0.5 mM diamide and 0.2 mM GSH. The thionylated PKC exhibited slightly retarded migration with an apparent molecular weight of ~85 kDa, which is larger than the unmodified form (82 kDa). The extent of thionylation by 0.4 mM GS-DSMO was much less than that by GS-DSDO, and thionylation by the same concentration of GSNO or GSSG was negligible. It should be noted that the PKC detected by the PKC antibody in the 0.4 mM GS-GSMO-treated sample was significantly less than the others due to aggregation of the kinase, which was poorly resolved in a nonreducing SDS gel (Figure 6C, upper left panel).

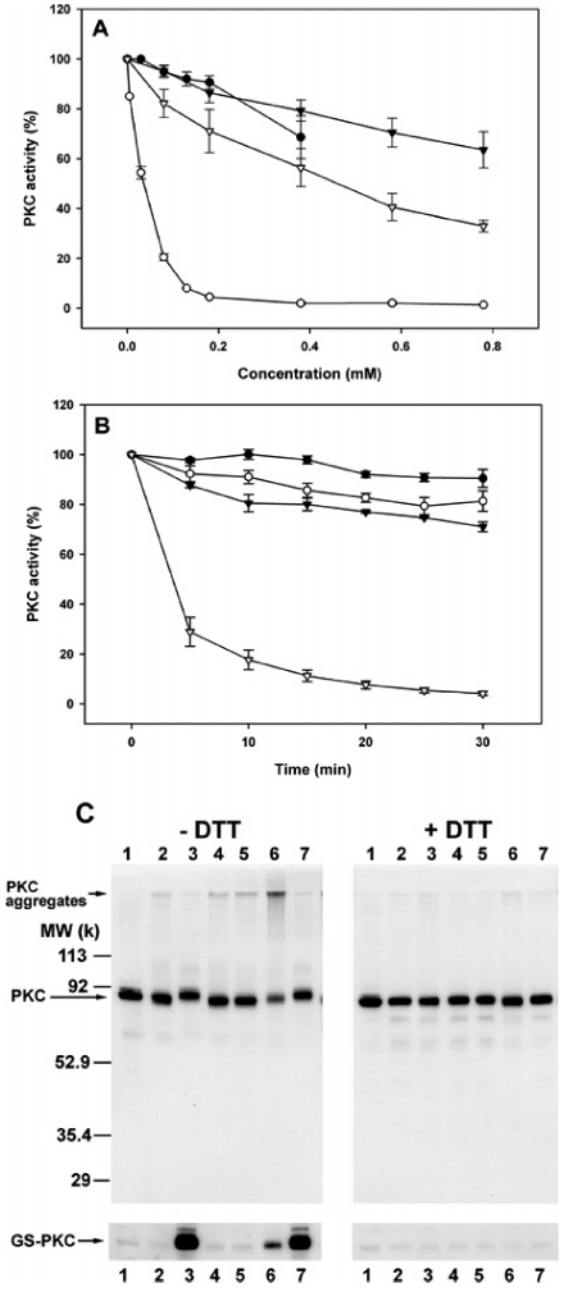

FIGURE 6: Inactivation of PKC by DSMO and DSDO. (A) Conventional PKCs ($\alpha + \beta + \gamma$) preparation in 10 mM potassium phosphate buffer, pH 7.5, containing 10% glycerol was incubated with increasing concentrations of CPS-DSMO (▼), CPS-DSDO (▽), GS-DSMO (●), and GS-DSDO (○) for 5 min at 30 °C, and the kinase activity was determined with Ca^{2+}/PS/DG. (B) Time course of PKC inactivation without oxidant (●) or that mediated by 0.1 mM GS-DSDO (▽), 0.4 mM GSSG (○), and 0.4 mM GSNO (▼). The activity measured at zero time without oxidant was set at 100%. (C) Glutathionylation detected by antibody against GS-associated protein. PKC (~1 μg) was incubated without (lane 1) or with 0.4 mM each of GSSG (lane 2); 0.5 mM diamide + 0.2 mM GSH (lane 3); 0.4 mM GSNO (lane 4); 0.1 mM GS-DSMO(lane 5); 0.4 mM GS-DSMO (lane 6); and 0.1 mM GS-DSDO (lane 7) for 5 min in duplicate, and the reactions were either terminated by addition of iodoacetamide (13 mM) (left panel) or with 10 mM DTT followed by the addition of iodoacetamide (13 mM) (right panel). Samples were resolved by 8−16% nonreducing SDS−PAGE, transferred to nitrocellulose membrane, and blotted with antibody to detect PKC (upper panels) or GS-associated PKC (GS-PKC) (lower panels).

When the modified PKC was reduced by DTT, no immunoreactive band was seen with the GS-protein specific antibody,

while all the PKC antibody-positive bands migrated uniformly as 82 kDa protein with nearly equal intensity (Figure 6C, right panels).

To determine the stoichiometry of thionylation, PKC β was incubated with [^{35}S]GS-DSDO at 0.1 and 0.2 mM for 30 min. The estimated stoichiometry of thionylation was 4−5 mol/mol PKC β (4.6 ± 0.49 mol/mol, $n = 9$) with three separate kinase preparations. Tryptic digestion of the thionylated PKC revealed at least four sites being modified by GS-DSDO, including three in the regulatory domain (QGFQC^{67}QVC^{70}C^{71}FVVHK, $m/z = 1928$, containing one GS; RC^{78}HEFVTFSC^{86}PGADKGPASDDPR, $m/z = 2946$, containing one GS; and C^{217}SLNPEWNETFR, $m/z = 1928$, containing one GS) and one in the catalytic domain (LGC^{586}GQEGER, $m/z = 1222$, containing one GS). The precise site of thionylation in the zinc fingers (C^{67}, C^{70}, C^{71}, C^{78}, and C^{86}) within the regulatory domain has not been determined. Also, the site of thionylation mediated by GS-DSMO was not determined due to a relatively low stoichiometry in the presence of 0.4 mM [^{35}S]GS-DSMO (1.25 ± 0.2 mol/mol, $n = 4$) and the tendency of the modified PKC β to form aggregates.

Incubation of PKC β with GS-DSDO resulted in glutathionylation and inactivation of the kinase without causing an increase in the Ca^{2+}/PS/DG-independent activity (Figure 7A). This is in contrast to those seen in the superoxide- and H_2O_2-induced modifications of PKC, in which the autonomous activity without activators is increased (*24*, *25*). Inactivation of PKC by GS-DSDO could be reversed by DTT at a low level of thionylation; addition of Zn^{2+} (50 μM) slightly improved the reversibility by DTT. It became less reversible as the extent of inactivation progressively increased (Figure 7A). The completely inactivated kinase could not be reactivated either by 10 mM GSH, 10 mM GSH + 10 μM glutaredoxin, or thioredoxin reductase (15 mU) + 1.6 mM NADPH + 8 μM thioredoxin (data not shown). The lack of reversibility of the kinase activity in the extensively thionylated PKC (>3 mol/mol) by reducing agents, such as DTT and GSH, was not due to the inability of these agents to release the GSH moiety from the kinase. In fact, the [^{35}S]GS-moiety was almost completely released from the thionylated PKC by 10 mM DTT + 50 μM Zn^{2+} (Figure 7B). At a lower level of thionylation (<2 mol/mol), the inactivated PKC was readily reversed by the reducing agent with a concomitant release of GSH.

Differential Susceptibility of the GS-DSMO- and GS-DSDO-Modified PKC to Limited Proteolysis. To determine the structural changes resulting from modification of PKC by GS-DSMO and GS-DSDO, ^{35}S-labeled PKC β was subjected to limited proteolysis by trypsin (Figure 8). Native PKC can be cleaved at the hinge region to generate a 45−48 kDa catalytic and a 33−38 kDa regulatory domain (*12*). Interestingly, the kinase modified by GS-DSDO was very susceptible to proteolysis (panels B and D) as compared to that modified by GS-DSMO (panels A and C), and the patterns of the resulting proteolytic fragments were distinct between them. Both the catalytic and the regulatory domains of the GS-DSMO-treated PKC β could be identified by autoradiography (panel A) and immunoblot with a polyclonal antibody against PKC (panel C), suggesting that the modified kinase exhibits similar susceptibility to proteolysis as the native kinase. The extent of thionylation at the regulatory

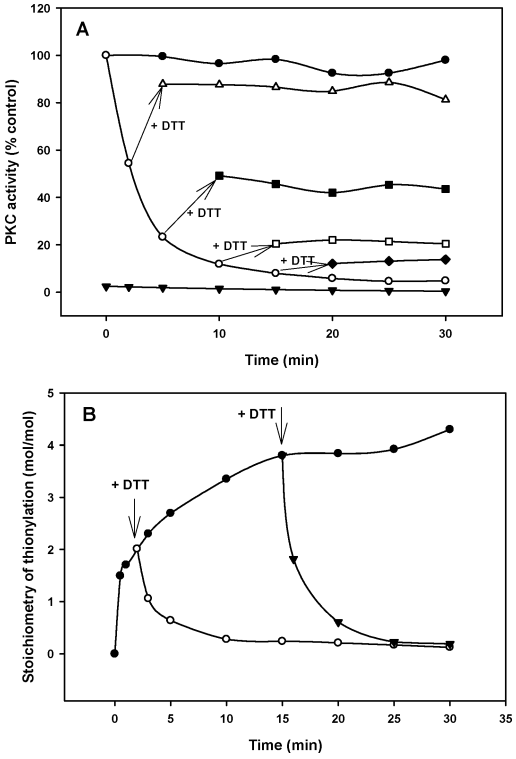

FIGURE 7: Reversibility of the GS-DSDO-mediated inactivation of PKC by DTT/Zn^{2+}. (A) PKC (~1 μg in 10 mM potassium phosphate buffer, pH 7.5, containing 10% glycerol) was incubated with 80 μM GS-DSDO, and samples were taken at timed intervals for assay of the kinase activity with (○) or without Ca^{2+}/PS/DG (▼). After 2 (△), 5 (■), 10 (□), and 15 min (◆) of incubation with GS-DSDO, aliquots of the reaction mixture were taken and supplemented with 10 mM DTT + 50 μM $ZnSO_4$ for measuring the kinase activity with Ca^{2+}/PS/DG. Kinase activity without addition of GS-DSDO was used as control (●), and its activity at zero time was set as 100%. (B) PKC (36 μg) was incubated in 0.12 mL of buffer (10 mM potassium phosphate, pH 7.5, containing 10% glycerol) with 80 μM [^{35}S]GS-DSDO at room temperature. At the indicated times, reaction was terminated by addition of iodoacetamide (2 mM), TCA (20%), and 100 μg of BSA as carrier for protein precipitation to measure [^{35}S]-incorporation. To determine the reversibility, aliquots were taken after 2 (○) and 15 min (▼) incubation with GS-DSDO and were added with DTT (10 mM) + $ZnSO_4$ (50 μM). Samples were taken at different times for measurement of [^{35}S]-incorporation into protein.

domain was approximately 1.5-fold greater than that of the catalytic domain following incubation of PKC β with 0.4 mM [^{35}S]GS-DSMO with a stoichiometry of ~1.2 mol/mol. The trypsinization patterns of the GS-DSDO-treated PKC with a stoichiometry of ~5 mol/mol were different from those of the GS-DSMO-treated one. The catalytic domain of PKC was not detectable in the GS-DSDO-treated sample even after merely 1 min of tryptic digestion, although the regulatory domain was identifiable by autoradiography (Figure 8B) and by immunoblot (panel D). There were several lower molecular weight fragments formed after tryptic digestion, which presumably were derived from both the catalytic and the regulatory domains. These results suggest that thionylation mediated by GS-DSDO induces extensive conformational changes at the catalytic and regulatory domains so that numerous sites become susceptible to tryptic digestion.

GS-DSDO and CPS-DSDO Exhibit Different Specificities toward PKC. Incubation of PKC with GS-DSMO, GS-

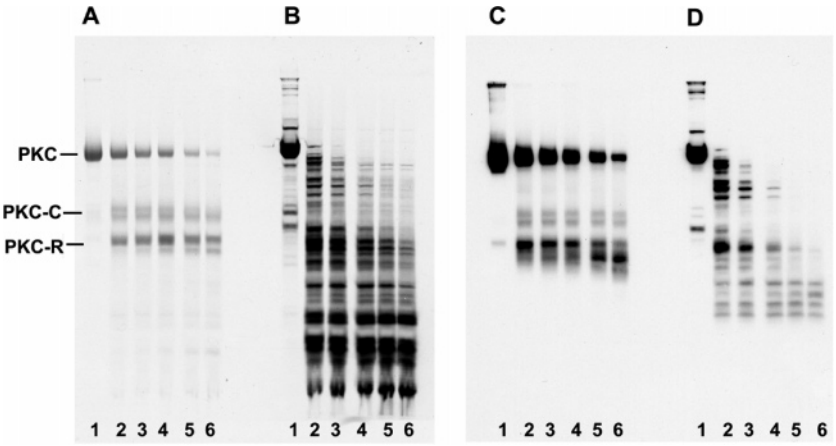

FIGURE 8: Thionylation of PKC β by [^{35}S]-labeled GS-DSMO and GS-DSDO and the susceptibility of the thionylated kinase to limited trypsinization. Freshly reduced PKC β (~15 μg) was incubated with 0.4 and 0.1 mM each of [^{35}S]-labeled GS-DSMO (A and C) and GS-DSDO (B and D), respectively, in 50 μL of reaction mixture containing 10 mM potassium phosphate buffer, pH 7.5, and 10% glycerol at room temperature for 30 min. Before treatment with trypsin, aliquots (containing ~2 μg of PKC β) were taken as zero time control (lane 1 in all panels). The remaining reaction mixtures were incubated with trypsin (1/80 of the amount of PKC) and samples (~2 μg PKC β) were taken after incubation for 1 (lane 2), 2 (lane 3), 3 (lane 4), 5 (lane 5), and 10 min (lane 6), and trypsinization was terminated with soybean trypsin inhibitor (20 μg). Reaction mixtures were resolved by nonreducing 8−16% SDS−PAGE, transferred to nitrocellulose membrane for autoradiography (A and B), and immunoblot with polyclonal PKC antibody that recognizes both the catalytic and the regulatory domains of PKC (C and D).

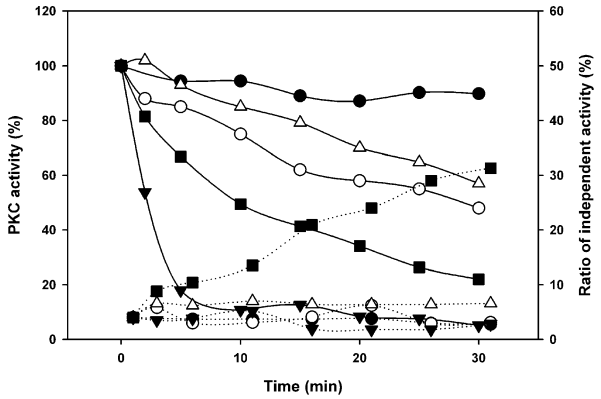

FIGURE 9: Thionylation of PKC mediated by GS-DSDO and CPS-DSDO resulted in differential effects on the activator-independent activity. PKCs ($\alpha + \beta + \gamma$) preparation was incubated without addition of oxidant (●) or with 80 μM GS-DSDO (▼), 0.4 mM each of GS-DSMO (○), CPS-DSMO (△), and CPS-DSDO (■), and samples were taken at timed intervals for assay of PKC activity with Ca^{2+}/PS/DG or 2 mM EGTA without activator. Kinase activity with Ca^{2+}/PS/DG (solid lines) at zero time in sample without oxidant was set as 100% and the ratio of independent activity (+EGTA/+activators) (dotted lines) was calculated for each time point.

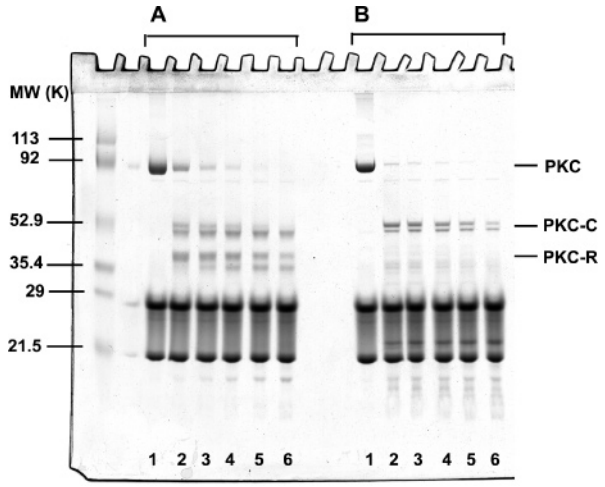

FIGURE 10: Limited trypsinization of CPS-DSMO- and CPS-DSDO-treated PKC β. Freshly reduced PKC β (~15 μg) was incubated with 0.4 mM each of CPS-DSMO (A) or CPS-DSDO (B) in 50 μL of reaction mixture containing 10 mM potassium phosphate buffer, pH 7.5, and 10% glycerol at room temperature for 30 min. After the reaction, samples (~2 μg of PKC β) were taken before treatment with trypsin (lane 1 in all panels) as zero time control. The remaining mixtures were treated with trypsin (1/80 of the amount of PKC) for 1 (lane 2), 2 (lane 3), 3 (lane 4), 5 (lane 5), and 10 min (lane 6), and trypsinization was terminated with soybean trypsin inhibitor (20 μg). Reaction mixtures were resolved by nonreducing 8−16% SDS−PAGE and stained with Coomassie blue. Those heavy protein bands of molecular weight lower than 29 kDa were derived from the added trypsin inhibitor.

DSDO, and CPS-DSMO caused inactivation of PKC activity measured in the presence of activators, Ca^{2+}/PS/DG, without a significant effect on the activator-independent activity measured in the presence of EGTA (Figure 9). In contrast, treatment of PKC with CPS-DSDO resulted in an increase in the percent of independent activity. These results suggest that CPS-DSDO modifies PKC distinctively from those by the other DSOs. To confirm this prediction, PKC β was treated with CPS-DSMO and CPS-DSDO and subjected to limited proteolysis (Figure 10). Digestion of the CPS-DSMO-treated PKC (Figure 10A) resulted in the formation of the catalytic and regulatory domains revealed by staining of the protein with Coomassie blue; these patterns were similar to those of the GS-DSMO-treated PKC. Interestingly, unlike the GS-DSDO-treated PKC, the regulatory domain of the CPS-DSDO-treated kinase (Figure 10B) was more susceptible to proteolysis than the catalytic domain. The heavy Coomassie blue-stained protein bands with molecular weights ranging from 29 to 21 kDa in all samples were derived from the added trypsin inhibitor. These results suggest that the regulatory domain of PKC is modified by CPS-DSDO in such a manner so that multiple sites are exposed to tryptic digestion. These results demonstrate that CPS-DSDO and GS-DSDO have distinct specificity toward different PKC domains.

DISCUSSION

Recently, DSMO and DSDO were proposed as potential signaling molecules of reactive sulfur species because of their generation in the oxidant-treated brain slices and their high reactivity toward protein sulfhydryl group (*4*, *26*−*28*). The mechanism for the synthesis of these compounds in vivo is still unknown. Here, we showed that both DSMO and DSDO can be prepared in bulk quantity with high purity by oxidation of thiols with H_2O_2 using iron or MTO as catalyst. It is generally believed that oxidation of thiol by H_2O_2 in the presence of iron involves the formation of a hydroxyl radical, •OH, which reacts with thiol to form thiyl radical and then disulfide (*18*). Further oxidation of disulfide generates DSOs, sulfinic acid, and sulfonic acid. However, based on the kinetics of thiol oxidation in the presence of iron to form DSMO (monitored at 244 nm) (Figure 1), we noticed that the rate of oxidation of GSH was much faster than that of GSSG, suggesting that DSMO is the initial product of thiol oxidation rather than the secondary reaction product of oxidation of GSSG. Thiol reduces Fe^{3+} to Fe^{2+} and forming thiyl radical (*29*) and the resulting Fe^{2+} catalyzes the decomposition of H_2O_2 to generate reactive intermediate peroxo ($Fe^{2+}OOH$) (*30*) or iron (IV)-oxo (FeO^{2+}) species (*31*) and •OH and •OOH radicals (*32*) by the Fenton reaction. These radicals can also react with thiol to form the thiyl radical. It seems that the thiyl radical reacts with the iron peroxo and iron-oxo intermediate and/or •OH and •OOH radicals to generate DSOs. In the Fe^{2+}/thiol/H_2O_2 system, thiyl radical and •OH are also formed (*33*, *34*). In this case, the thiyl radical is generated by •OH-mediated oxidation of thiol. The MTO-catalyzed oxidation of thiols by H_2O_2 is believed to be initiated by nucleophilic attack of the sulfur atom at the oxygen atom of mono- or di-peroxorhenium complexes (*14*). Transfer of one oxygen to the sulfur atom of thiol generates sulfenic acid and transfer of two oxygen atoms becomes sulfinic acid. Condensation of two sulfenic acids produces DSMO and that of sulfenic and sulfinic acids generates DSDO. Alternatively, further oxidation of DSMO by peroxorhenium could also produce DSDO. Formation of DSOs by direct oxidation of thiol is kinetically more favorable than that of disulfide by MTO/H_2O_2 (Figure 1). We speculate that in vivo DSOs may be generated by those reactions catalyzed by cytochrome P-450 (*35*−*38*) and flavin-containing monooxygenases (*35*, *38*, *39*), which are known to transfer activated oxygen to sulfur atom. Furthermore, sulfur-centered radicals of higher oxidative states such as sulfinyl (RSO•), sulfonyl (RSO_2•), and thiol peroxy (RSOO•) radicals are generated by reaction of thiyl radicals with molecular oxygen (*40*, *41*). Sulfinyl radicals are also generated by oxidation of thiol with superoxide (*42*, *43*) and with peroxynitrite in the presence of carbon dioxide (*44*). Reaction of thiyl radical with sulfinyl and sulfonyl radicals could also generate DSMO and DSDO.

Oxidant-induced thionylation of proteins is a widespread biological phenomenon in various cellular compartments, yet mechanisms of these modifications are not entirely clear. Chemically synthesized DSOs are useful reagents for the characterization of the alteration of protein function resulting from thionylation by a variety of thiols. The distinct specificity inherent among DSOs derived from different thiols could contribute to a broad range of cellular responses analogous to those mediated by different protein kinase-catalyzed phosphorylation. Previously, tubulin (*23*) and glyceralehyde 3-phosphate dehydrogenase (*15*, *21*, *45*, *46*) have been shown to be potential targets of glutathionylation, and their thionylation can be replicated by treatment with either GS-DSMO or GS-DSDO. Since the currently available method for the characterization of thionylated protein is still limited, application of radioactive DSOs will facilitate the identification of target proteins and their sites of modification. Previously, the Ca^{2+}/PS/DG-activated PKCs were shown to be thionylated by a combination of thiol-specific oxidant diamide and glutathione and resulted in an inactivation of the kinase (*47*, *48*). Both the regulatory and catalytic domains of PKC contain several cysteine residues susceptible to modification by DSOs. For these conventional PKCs, the two zinc fingers in the regulatory domain each contain six regularly spaced cysteine residues that fold to coordinate two zinc atoms (*49*) and the catalytic domain contains several cysteine residues that are not coordinated with metal and are free to react with modifier. Oxidative modification of the regulatory domain frequently causes an increase in the autonomous activity of PKC, whereas that of the catalytic domain induces inactivation of the kinase activity (*50*). Even though the regulatory domain of PKC was thionylated by GS-DSDO, there was no increase in the autonomous activity. In contrast, PKC treated with CPS-DSDO resulted in a significant increase in the activator-independent activity. These findings suggest that different thiol-containing compounds, when converted into their respective DSDOs, may have distinct regulatory functions through thionylation of proteins. It also implies that thiol-containing drugs, e.g., CPSH, and DSO-containing natural products, e.g., allicin derived from garlic and S-methyl methanethiosulfonate ($CH_3S(O)_2SCH_3$) derived from cauliflower and cabbage, may function as thionylating agents in accounting for their beneficial health effects.

Using PKC β (containing 21 cysteine residues) as a representative member of the conventional PKCs for detailed analysis, we showed that this kinase was thionylated by [^{35}S]GS-DSDO up to a stoichiometry of 4−5 mol/mol, whereas GS-DSMO only achieved an incorporation of approximately 1 mol/mol. Similar respective degrees of thionylation of PKC α and γ (containing 20 and 22 cysteine residues, respectively) as PKC β were also observed by these two compounds. The stoichiometry of thionylation mediated by DSOs derived from CPSH has not been determined. It is surprising that DSMO and DSDO have such a difference in the stoichiometry of the thionylation of PKC since only the exposed cysteine residues are susceptible to thionylation by these compounds. It is likely that the $RS(O)_2$-functional group has a greater accessibility to those cysteine residues as compared to the RS(O)-group. Since the GS-DSMO-treated PKC has a tendency to from aggregates, it appears that the initial thionylation causes a subsequent formation of inter- or intramolecular disulfide and thus results in a low stoichiometry of thionylation. Although thionylation of PKC β by GS-DSDO and CPS-DSDO increases the susceptibility of the kinase to limited proteolysis, these two compounds may cause different structural changes in the kinase; as a result, the catalytic and regulatory domains of the GS- and CPS-thionylated kinase exhibit different susceptibility to proteolysis. The effects of GS-DSMO and CPS-DSMO on PKC

are, however, comparable based on their inhibition of the kinase activity as well as their effects on the modified kinase during limited proteolysis. Since the DSDO-mediated thionylation of PKC greatly enhances its susceptibility to degradation by protease, we propose that this process may also contribute to the oxidant-mediated proteolysis in cells (*51*). DSDO with its higher oxidative state could serve as a signal molecule to trigger proteolytic degradation of protein under oxidative stress. The diverse effects of various reactive sulfur species toward PKC may serve as a prototype for the design of drugs to target a specific group of proteins for therapeutic application.

The current study extended our previous findings that GS-DSMO and GS-DSDO were potential cellular modifiers of neurogranin, a small molecular weight protein (7.5 kDa) of little structural feature, for redox regulation of its function (*4*). Using a structurally more complex molecule such as PKC for investigating the structural and functional relationship after modification by DSOs, we have illustrated here several intricate effects of these compounds on PKC resulting from their unique specificities toward the different PKC domains. The efficacies of DSOs in modifying protein sulfhydryl group were significantly greater than those of GSSG and GSNO, and these DSOs are likely mediators of oxidants, such as H_2O_2, superoxide, nitric oxide, and peroxynitrite generated in vivo. The same implication is also applicable to other sulfhydryl compounds, which are converted to their respective DSOs for the modification of protein. Considering the widespread presence of sulfur-containing compounds in biological systems and in the environment, the reactive sulfur species must play a broad range of oxidant-regulated cellular responses.

REFERENCES

1. Shackelford, R. E., Heinloth, A. N., Heard, S. C., and Paules, R. S. (2005) Cellular and molecular targets of protein S-glutathiolation, *Antioxid. Redox Signaling 7*, 940−950.
2. Klatt. P., and Lamas, S. (2000) Regulation of protein function by S-glutathiolation in response to oxidative and nitrosative stress, *Eur. J. Biochem. 267*, 4928−4944.
3. Mustacich, D., and Powis, G. (2000) Thioredoxin reductase, *Biochem. J.* 346, Pt 1, 1−8.
4. Li, J., Huang, F. L., and Huang, K. P. (2001) Glutathiolation of proteins by glutathione disulfide S-oxide derived from S-nitrosoglutathione. Modifications of rat brain neurogranin/RC3 and neuromodulin/GAP-43, *J. Biol. Chem. 276*, 3098−3105.
5. Nakamura, Y., Nakamura, Y. K., Tashiro, S., Mukai, K., and Tomita, I. (1998) Modification of enzyme sulfhydryl groups suppresses UV-induced mutagenesis depending on the nucleotide excision repair system in Escherichia coli B/r WP2, *Mutat. Res. 407*, 47−53.
6. Nakamura, Y, Matsuo, T., Shimoi, K., and Tomita, I. (1993) S-methyl methane thiosulfonate, a new antimutagenic compound isolated from Brassica oleracea L. var. botrytis, *Biol. Pharm. Bull. 16*, 207−209.
7. Kawamori, T., Tanaka, T., Ohnishi, M., Hirose, Y., Nakamura, Y., Satoh, K., Hara, A., and Mori, H. (1995) Chemoprevention of azoxymethane-induced colon carcinogenesis by dietary feeding of S-methyl methane thiosulfonate in male F344 rats, *Cancer Res. 55*, 4053−4058.
8. Kyung, K. H., and Fleming, HP. (1997) Antimicrobial activity of sulfur compounds derived from cabbage, *J. Food Protein 60*, 67−71.
9. Van Antwerpen, P., Legssyer, I., Zouaoui, Boudjeltia, K., Babar, S., Moreau, P., Moguilevsky, N., Vanhaeverbeek, M., Ducobu, J., and Neve, J. (2006) Captopril inhibits the oxidative modification of apolipoprotein B-100 caused by myeloperoxydase in a comparative in vitro assay of angiotensin converting enzyme inhibitors, *Eur. J. Pharmacol. 537*, 31−36.
10. Narazaki, R., Harada, K., Sugii, A., and Otagiri, M. (1997) Kinetic analysis of the covalent binding of captopril to human serum albumin, *J. Pharm. Sci. 86*, 215−219.
11. Huang, K. P., Huang, F. L., and Chen, H. C. (1993) Characterization of a 7.5-kDa protein kinase C substrate (RC3 protein, neurogranin) from rat brain, *Arch Biochem Biophys. 305*, 570−580.
12. Huang, K. P., and Huang, F. L. (1986) Immunochemical characterization of rat brain protein kinase C, *J. Biol. Chem. 261*, 14781−14787.
13. Huang, K. P., Nakabayashi, H., and Huang, F. L. (1986) Isozymic forms of rat brain Ca2+-activated and phospholipid-dependent protein kinase, *Proc. Natl. Acad. Sci.* U.S.A. *83*, 8535−8539.
14. Wang, Y., and Espenson, J. H. (2000) Oxidation of symmetric disulfides with hydrogen peroxide catalyzed by methyltrioxorhenium(VII), *J. Org. Chem. 65*, 104−107.
15. Tao, L., and English, A. M. (2004) Protein S-glutathiolation triggered by decomposed S-nitrosoglutathione, *Biochemistry 43*, 4028−4038.
16. Calam, D. H., and Waley, S. G. (1962) Some derivatives of glutathione, *Biochem. J. 85*, 417−419.
17. Steinman, H. M., and Richards, F. M. (1970) Participation of cysteinyl residues in the structure and function of muscle aldolase. Characterization of mixed disulfide derivatives, *Biochemistry 9*, 4360−4372.
18. Oae, S., and Doi, J. T. (1991) *Organic Sulfur Chemistry: Structure and Mechanism*; CRC Press: Boca Raton, Fla.
19. Finley, J. W., Wheeler, E. L., and Witt, S. C. (1981) Oxidation of glutathione by hydrogen peroxide and other oxidizing agents, *J. Agric. Food Chem. 29*, 404−407.
20. Brown, K. N., and Espenson, J. H. (1996) Stepwise oxidation of thiophene and its derivatives by hydrogen peroxide catalyzed by methyltrioxorhenium(VII), *Inorg. Chem. 35*, 7211−7216.
21. Giles, G. I., Tasker, K. M., Collins, C., Giles, N. M., O'Rourke, E., and Jacob, C. (2002) Reactive sulphur species: an in vitro investigation of the oxidation properties of disulphide S-oxides, *Biochem. J. 364*, 579−585.
22. Eaton, P., Wright, N., Hearse, D. J., and Shattock, M. J. (2002) Glyceraldehyde phosphate dehydrogenase oxidation during cardiac ischemia and reperfusion, *J. Mol. Cell Cardiol. 34*, 1549−1560.
23. Landino, L. M., Moynihan, K. L., Todd, J. V., and Kennett, K. L. (2004) Modulation of the redox state of tubulin by the glutathione/glutaredoxin reductase system, *Biochem. Biophys. Res. Commun. 314*, 555−560.
24. Gopalakrishna, R., and Anderson, W. B. (1989) Ca2+- and phospholipid-independent activation of protein kinase C by selective oxidative modification of the regulatory domain, *Proc. Natl. Acad. Sci. U.S.A. 86*, 6758−6762.
25. Knapp, L. T., and Klann, E. (2000) Superoxide-induced stimulation of protein kinase C via thiol modification and modulation of zinc content, *J. Biol. Chem. 275*, 24136−24145.
26. Huang, K. P., and Huang, F. L. (2002) Glutathionylation of proteins by glutathione disulfide S-oxide, *Biochem. Pharmacol. 64*, 1049−1056.
27. Giles, G. I., and Jacob, C. (2002) Reactive sulfur species: an emerging concept in oxidative stress, *Biol. Chem. 383*, 375−388.
28. Jacob, C., Lancaster, J. R., and Giles, G. I. (2004) Reactive sulphur species in oxidative signal transduction, *Biochem. Soc. Trans. 32*, 1015−1017.
29. Misik, V., Mak, I. T., Stafford, R. E., and Weglicki, W. B. (1993) Reactions of captopril and epicaptopril with transition metal ions and hydroxyl radicals: an EPR spectroscopy study, *Free Radical Biol. Med. 15*, 611−619.
30. Wink, D. A., Nims, R. W., Saavedra, J. E., Utermahlen, W. E., Jr., and Ford, P. C. (1994) The Fenton oxidation mechanism: reactivities of biologically relevant substrates with two oxidizing intermediates differ from those predicted for the hydroxyl radical, *Proc. Natl. Acad. Sci. U.S.A. 91*, 6604−6608.
31. Buda, F., Ensing, B., Gribnau, M. C., and Baerends, E. J. (2001) DFT study of the active intermediate in the Fenton reaction, *Chemistry 7*, 2775−2783.
32. Buda, F., Ensing, B., Gribnau, M. C., and Baerends, E. J. (2003) O2 evolution in the Fenton reaction, *Chemistry 9*, 3436−3444.
33. Hanna, P. M., and Mason, R. P. (1992) Direct evidence for inhibition of free radical formation from Cu(I) and hydrogen

peroxide by glutathione and other potential ligands using the EPR spin-trapping technique, *Arch. Biochem. Biophys. 295*, 205−213.
34. Spear, N., and Aust, S. D. (1995) Effects of glutathione on Fenton reagent-dependent radical production and DNA oxidation, *Arch. Biochem. Biophys. 324*, 111−116.
35. Teyssier, C., Guenot, L., Suschetet, M., and Siess, M. H. (1999) Metabolism of diallyl disulfide by human liver microsomal cytochromes P-450 and flavin-containing monooxygenases, *Drug Metab. Dispos. 27*, 835−841.
36. Coon, M. J. (2005) Cytochrome P450: Nature's most versatile biological catalyst, *Annu. Rev. Pharmacol. Toxicol. 45*, 1−25.
37. Fukushima, D., Kim, Y. H., Iyanagi, T., and Oae, S. (1978) Enzymatic oxidation of disulfides and thiolsulfinates by both rabbit liver microsomes and a reconstituted system with purified cytochrome P-450, *J. Biochem. (Tokyo) 83*, 1019−1027.
38. Germain, E., Chevalier, J., Siess, M. H., and Teyssier, C. (2003) Hepatic metabolism of diallyl disulphide in rat and man, *Xenobiotica 33*, 1185−1199.
39. Cashman, J. R. (2000) Human flavin-containing monooxygenase: substrate specificity and role in drug metabolism, *Curr. Drug Metab. 1*, 181−191.
40. Sevilla, M. D., Becker, D., and Yan, M. (1990) The formation and structure of the sulfoxyl radicals RSO(.), RSOO(.), RSO2(.), and RSO2OO(.) from the reaction of cysteine, glutathione and penicillamine thiyl radicals with molecular oxygen, *Int. J. Radiat. Biol. 57*, 65−81.
41. Sevilla, M. D., Becker, D., Swarts, S., and Herrington, J. (1987) Sulfinyl radical formation from the reaction of cysteine and glutathione thiyl radicals with molecular oxygen, *Biochem. Biophys. Res. Commun. 144*, 1037−1042.
42. Winterbourn, C. C., and Metodiewa, D. (1994) The reaction of superoxide with reduced glutathione, *Arch. Biochem. Biophys. 314*, 284−290.
43. Winterbourn, C. C., and Metodiewa, D. (1999) Reactivity of biologically important thiol compounds with superoxide and hydrogen peroxide, *Free Radical Biol. Med. 27*, 322−328.
44. Bonini, M. G., and Augusto, O. (2001) Carbon dioxide stimulates the production of thiyl, sulfinyl, and disulfide radical anion from thiol oxidation by peroxynitrite, *J. Biol. Chem. 276*, 9749−9754.
45. Klatt, P., Pineda, Molina, E., Perez-Sala, D., and Lamas, S. (2000) Novel application of S-nitrosoglutathione-Sepharose to identify proteins that are potential targets for S-nitrosoglutathione-induced mixed-disulphide formation, *Biochem. J. 349*, 567−578.
46. Eaton, P., Byers, H. L., Leeds, N., Ward, M. A., and Shattock, M. J. (2002) Detection, quantitation, purification, and identification of cardiac proteins S-thiolated during ischemia and reperfusion, *J. Biol. Chem. 277*, 9806−9811.
47. Chu, F., Ward, N. E., and O'Brian, C. A. (2001) Potent inactivation of representative members of each PKC isozyme subfamily and PKD via S-thiolation by the tumor-promotion/progression antagonist glutathione but not by its precursor cysteine, *Carcinogenesis 22*, 1221−1229.
48. Ward, N. E., Stewart, J. R., Ioannides, C. G., and O'Brian, C. A. (2000) Oxidant-induced S-glutathiolation inactivates protein kinase C-alpha (PKC-alpha): a potential mechanism of PKC isozyme regulation, *Biochemistry 39*, 10319−10329.
49. Quest, A. F., Bloomenthal, J., Bardes, E. S., and Bell, R. M. (1992) The regulatory domain of protein kinase C coordinates four atoms of zinc, *J. Biol. Chem. 267*, 10193−10197.
50. Gopalakrishna, R., and Jaken, S. (2000) Protein kinase C signaling and oxidative stress, *Free Radical Biol. Med. 28*, 1349−1361.
51. Grune, T., Reinheckel, T., and Davies, K. J. (1997) Degradation of oxidized proteins in mammalian cells, *FASEB J. 11*, 526−534.

BI061955I